Effect of Soluble Nickel on Cellular Energy Metabolism in A549 Cells

HAOBIN CHEN AND MAX COSTA[1]

Nelson Institute of Environmental Medicine, New York University School of Medicine, Tuxedo, New York 10987

Iron is an essential nutrient to most organisms, and is actively involved in oxygen delivery, electron transport, DNA synthesis, and many other biochemical reactions important for cell survival. We previously reported that nickel (Ni) ion exposure decreases cellular iron level and converts cytosolic aconitase (c-aconitase) to iron-regulatory protein-1 in A549 cells (Chen H, Davidson T, Singleton S, Garrick MD, Costa M. Toxicol Appl Pharmacol 206:275–287, 2005). Here, we further investigated the effect of Ni ion exposure on the activity of mitochondrial iron-sulfur (Fe-S) enzymes and cellular energy metabolism. We found that acute Ni ion treatment up to 1 m*M* exhibits minimal toxicity in A549 cells. Ni ion treatment decreases the activity of several Fe-S enzymes related to cellular energy metabolism, including mitochondrial aconitase (m-aconitase), succinate dehydrogenase (SDH), and NADH:ubiquinone oxidoreductase (complex I). Low doses of Ni ion for 4 weeks resulted in an increased cellular glycolysis and NADH to NAD^+ ($NADH/NAD^+$) ratio, although glycolysis was inhibited at higher levels. Collectively, our results show that Ni ions decrease the activity of cellular iron (Fe)-containing enzymes, inhibit oxidative phosphorylation (OxPhos), and increase cellular glycolytic activity. Since increased glycolysis is one of the fundamental alterations of energy metabolism in cancer cells (the Warburg effect), the inhibition of Fe-S enzymes and subsequent changes in cellular energy metabolism caused by Ni ions may play an important role in Ni carcinogenesis. Exp Biol Med 231:1474–1480, 2006

Key words: Fe-S enzymes; $NADH/NAD^+$ ratio; glycolysis; oxidative phosphorylation

Introduction

Iron is an essential nutrient to most organisms, and is actively involved in oxygen delivery, electron transport, DNA synthesis, and many other biochemical reactions important for cell survival (1). However, excess free-available iron has the potential to harm the cell by generating reactive oxygen species through the Fenton reaction (2). To maintain an adequate iron level, the cell has developed sophisticated regulatory mechanisms, namely iron regulatory proteins (IRPs), to control the uptake, utilization, and storage of iron. IRP-1 and IRP-2 sense the level of free-available intracellular iron, and post-transcriptionally modulate the expression of genes that encode transferrin receptor (TfR) and ferritin by binding to the iron response elements (IREs) present in their mRNAs (3). When activated under an iron-depleted condition, IRPs stabilize TfR mRNA and block the synthesis of ferritin, and thus, favor iron uptake over storage. Conversely, when the iron level is high, downregulation of IRP activity results in enhanced translation of ferritin mRNA and decreased stability of TfR mRNA. IRP-2 is mainly degraded by the proteasome during iron-repletion, while IRP-1 is inactivated by receiving a [4Fe-4S] cluster and is converted to cytosolic aconitase (c-aconitase), an enzyme which has the same activity as its counterpart, mitochondrial aconitase (m-aconitase).

Glycolysis, the tricarboxylic acid (TCA) cycle, and oxidative phosphorylation (OxPhos) are central biochemical processes in cellular energy metabolism, and are linked to cellular iron homeostasis. For instance, the expression of several genes that encode glycolytic enzymes is upregulated by the transcription factor hypoxia inducible factor-1 alpha (HIF-1α), which is stabilized and transactivated by the inhibition of several Fe(II)-2-oxoglutarate–dependent dioxygenases under iron-deficient conditions (4). Moreover, the availability of cellular iron may affect the TCA cycle and OxPhos by modulating the gene expression and/or activity of several iron-sulfur (Fe-S) enzymes, including m-aconitase, succinate dehydrogenase (SDH), and NADH:ubiquinone oxidoreductase (complex I). Iron deficiency can not only directly inhibit the biosynthesis of Fe-S clusters, but it can also block m-aconitase protein synthesis in mammalian cells by causing IRPs to bind to the IRE in its mRNA 5′ untranslated region (5′-UTR). Interestingly, IREs or IRE-like elements have also been found in mRNAs that encode other Fe-S proteins in some eukaryotes. In *Drosophila melanogaster*, the 5′-UTR of SDH subunit b mRNA has an

This work was supported by grant ES00260, ES10344, and T32-ES07324 from the National Institute of Environmental Health Sciences, and CA16087 from the National Cancer Institute.

[1] To whom correspondence should be addressed at Nelson Institute of Environmental Medicine, New York University School of Medicine, 57 Old Forge Road, Tuxedo, NY 10987. E-mail: costam@env.med.nyu.edu or costam01@nyu.edu

1535-3702/06/2319-1474$15.00

IRE that mediates a similar response to iron deficiency as m-aconitase (5). Recently, it was reported that synthesis of the 75-kDa subunit of mitochondrial complex I may also be regulated by an IRE-like stem-loop structure in the 5′-UTR of its mRNA (6).

We previously reported that nickel (Ni) ion exposure for 24 hrs decreased cellular iron by about 40% and converted c-aconitase into IRP-1 in lung carcinoma A549 cells (7). These results prompted us to test the hypothesis that Ni ion exposure decreases the activity of other cellular iron-dependent enzymes, such as those with Fe-S clusters in the TCA cycle and OxPhos. We found that Ni ion exposure decreases m-aconitase, SDH and mitochondrial complex I activities, but increases the activities of two other TCA cycle enzymes that do not rely on iron for their function. The possible impact of Ni ion exposure on cellular energy metabolism was also assessed and is discussed in this manuscript.

Materials and Methods

Chemicals. All reagents were obtained from Sigma (St. Louis, MO) unless otherwise specified.

Cell Culture. Human lung carcinoma A549 cells were maintained in Ham's F-12 K medium (GIBCO BRL, Grand Island, NY) supplemented with 10% fetal bovine serum and 1% penicillin-streptomycin. Cells were passaged two to three times each week and kept at 37°C in a humidified 5% CO_2 atmosphere.

Colony Formation Assay. After trypsinization, 1×10^6 cells were seeded into each dish (100-mm diameter). Cells were allowed to attach overnight, and then exposed to different concentrations of nickel chloride ($NiCl_2$) for 24 hrs. Cells were rinsed twice with prewarmed medium and then trypsinized. After neutralizing with complete medium, the cell suspension was passed through a 40 μm Falcon nylon cell strainer (BD Biosciences, San Jose, CA) to eliminate cell clumps. Two hundred cells were then reseeded into each of three dishes (150-mm diameter), and grown for 2 weeks. Surviving colonies were stained with Giemsa stain and counted. All experiments were conducted in triplicate.

Aconitase and Glutathione Peroxidase Activity. Cytosolic and mitochondrial aconitase activities were measured as previously described (7). Cellular selenium-dependent glutathione peroxidase activity was measured using a Glutathione Peroxidase Cellular Activity Assay kit (Sigma). All experiments were conducted in triplicate.

Mitochondria Isolation. About 2×10^7 cells were collected and the cell pellet was resuspended in M buffer (250 m*M* sucrose, 2 m*M* Hepes, pH 7.4, 0.1 m*M* ethylene glycol bis[2-aminoethyl ether]-N,N,N′N′-tetraacetic acid [EGTA]). After lysis with a glass-Teflon homogenizer by upward and downward motion 10 times, the homogenate was centrifuged at 600 *g* for 6 min. The supernatant was transferred to a clean Eppendorf tube, and the pellet was resuspended, homogenized, and centrifuged again. The supernatant collected from two homogenizations was combined and centrifuged at 10,000 *g* for 10 min. The pellet was washed once and resuspended in the appropriate buffer for the following mitochondrial enzyme assays.

Isocitrate Dehydrogenase (IDH) and Malate Dehydrogenase (MDH) Activity. IDH and MDH activities were measured as previously described (8). In brief, mitochondria were resuspended in PBS with 0.1% Triton X-100, and sonicated twice by applying 10×1-sec pulse with a Branson Sonifier 450 (Branson Ultrasonics Co., Danbury, CT). After centrifugation at 14,000 *g* for 30 min, the supernatant was transferred to a clean Eppendorf tube. After measuring protein concentration using the Bio-Rad *DC* protein assay (Bio-Rad, Richmond, CA), 50 μg supernatant was used to measure IDH and MDH activity. For the IDH assay, each assay contained 100 m*M* Tris, pH 7.4; 2 m*M* $NADP^+$; 2 m*M* magnesium chloride ($MgCl_2$); and 5 m*M* isocitrate in a final volume of 1 ml. For the MDH assay, each assay contained 100 m*M* Hepes-Tris, pH 7.4; 0.16 m*M* NADH; and 0.13 m*M* oxaloacetate in a final volume of 1 ml. Enzyme activity was measured by following the linear absorbance change at 340 nm at 30°C for 30 min using a HTS 7000 Plate Reader (Perkin Elmer, Wellesley, MA). An extinction coefficient of 6.81 mM^{-1} was used for NADH. All experiments were conducted in triplicate.

Complex I (NADH:ubiquinone oxidoreductase) and II (SDH) Activity. Complex I activity was measured as described by Ben-Shachar *et al.* (9). Briefly, mitochondria were resuspended in hypotonic buffer (25 m*M* potassium phosphate, pH 7.4 and 5 m*M* $MgCl_2$), and freeze-thawed three times. The sample was subsequently sonicated by applying a 10×1-sec pulse with a Branson Sonifier 450. Eighty micrograms of mitochondrial suspension were used to measure complex I activity in 20 m*M* potassium phosphate, pH 7.2; 5 m*M* $MgCl_2$; 1 m*M* potassium cyanide (KCN); 0.14 m*M* NADH; and 50 μ*M* Coenzyme Q1 (Sigma) in the presence or absence of 20 μ*M* rotenone. Oxidation of NADH was followed at 340 nm for 5 min. Complex I activity is reported as the difference between the rate of NADH oxidation with and without rotenone. SDH activity was measured as described by Parker *et al.* (10). In brief, the pellet was resuspended in hypotonic buffer (25 m*M* potassium phosphate, pH 7.4 and 5 m*M* $MgCl_2$) and snap-frozen in liquid nitrogen. After quickly thawing in a room temperature water bath, samples were promptly chilled to 4°C. Thirty micrograms of mitochondrial suspension were used to measure SDH activity by following the succinate-dependent reduction of 2,6-dichlorophenol-indophenol (DCIP) at 590 nm with or without 10 m*M* malonate. An extinction coefficient of 19.1 mM^{-1} was used for DCIP. SDH activity is reported as the difference between the rate of DCIP reduction with and without malonate. All experiments were conducted in triplicate.

Glucose and Lactate Measurement. The concentration of glucose in the medium was measured using a

Glucose Assay kit (Sigma). The concentration of lactate in the medium was measured as previously described (11). To measure lactate concentration, 0.5 ml cell medium was collected in an Eppendorf tube and deproteinized with 315 µl 7% perchloric acid. After incubation on ice for 15 min, samples were centrifuged at 14,000 *g* for 5 min and the supernatant was collected and adjusted to pH 6.0 with 1 *M* potassium hydroxide (KOH). Samples were centrifuged to remove potassium perchlorate. Twenty microliters of supernatant were put into a 24-well plate and incubated with 80 µmol glycine buffer, pH 10.0, 10 units lactate dehydrogenase (Sigma), and 2 mg NAD^+ in a final volume of 1.0 ml. After incubation at 25°C for 1 hr, the concentration of lactate was measured as the change in O.D. at 340 nm. Lactate standard solutions were assayed simultaneously. All experiments were conducted in triplicate.

NADH and NAD^+ Measurement. The concentrations of cellular NADH and NAD^+ were measured as previously described (12). Cells were washed twice with ice cold PBS and lysed in 1 ml ice-cold extraction buffer (10 m*M* nicotinamide, 20 m*M* sodium bicarbonate [$NaHCO_3$], and 100 m*M* bisodium carbonate [Na_2CO_3]). The scraped lysate was frozen in a dry ice–ethanol bath, thawed quickly in a room temperature water bath, and then kept on ice. The samples were centrifuged once to eliminate insoluble material. The lysate was then diluted to 200 µg/ml. Twenty-microgram samples, in triplicate, were directly added into a 96-well plate, and total NAD (NADH + NAD^+) concentration was measured using a cycling assay as described by Jacobson *et al.* (13). Each assay contained 100 m*M* bicine, pH 7.8, 500 m*M* ethanol, 0.42 m*M* 3-(4,5-dimethylthiazolyl-2)-2,5-diphenyltetrazolium bromide (MTT) tetrazolium, 1.66 m*M* phenazine ethosulfate, 4.16 m*M* EDTA, 0.83 mg/ml bovine serum albumin, and 14 units alcohol dehydrogenase in a final volume of 200 µl. The amount of total NAD was measured as the O.D. change at 590 nm at 37°C for 5 min with a HTS 7000 Plate Reader. For NADH measurement, the lysate was incubated at 60°C for 30 min to destroy NAD^+, and promptly chilled to 4°C. Twenty-microgram samples, in triplicate, were used to measure NADH concentration with the same cycling assay used to measure NAD concentration. NADH standard solutions were assayed simultaneously. The ratio of NADH/NAD^+ was calculated based on the results of total NAD and NADH concentrations. All experiments were conducted in triplicate.

ATP Measurement. Intracellular ATP was measured using an ENLITEN ATP Assay System kit (Promega, Madison, WI). Cells were rinsed twice with ice cold PBS and intracellular ATP was extracted in 0.5% trichloroacetic acid. After centrifugation at 20,000 *g* for 5 min, the supernatant was collected for ATP measurement and the pellet was dissolved in 0.5 *N* sodium hydroxide (NaOH) for protein measurement. Prior to ATP measurement, the pH of the supernatant was adjusted to pH 7.75 by adding 40 volumes of 25 m*M* Tricine buffer (pH 7.8). The light intensity emitted after adding rL/L reagent (Promega) was determined using a luminometer (Wallac 1420 Victor multilabel counter system, Perkin Elmer), with a delay of 2 sec and integration time of 10 sec. All experiments were conducted in triplicate.

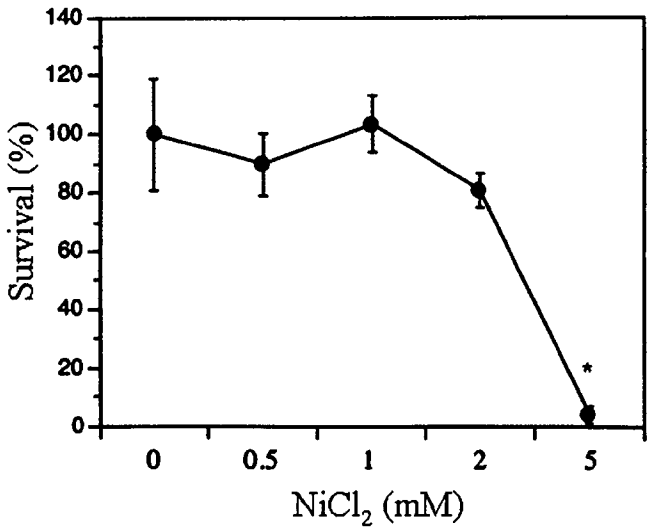

Figure 1. Cytotoxicity of $NiCl_2$ in A549 cells. Logarithmically growing A549 cells were treated with the indicated concentrations of $NiCl_2$ for 24 hrs, trypsinized, and reseeded for the determination of colony formation ability. *Statistically significant change ($P < 0.05$) when compared to controls.

Statistical Analysis. Two-tailed Student's *t* tests were used to determine the significance of differences in enzyme activity or metabolite concentration between treated samples and controls. Differences were considered significant at a $P < 0.05$.

Results

Toxicity of Ni Ion Exposure in A549 Cells. In contrast to many other transition metal ions, mammalian cells tolerate a high level of soluble nickel. To determine Ni ion toxicity in lung carcinoma A549 cells, we measured their clonogenic survival following Ni ion exposure. After treating cells with various concentrations of $NiCl_2$ for 24 hrs, equal numbers of A549 cells were reseeded and grown in complete medium in the absence of Ni ions. The number of colonies was counted 2 weeks later. As shown in Figure 1, the colonogenic rate of A549 cells was not affected by 1 m*M* Ni ions, but decreased by 20% at 2 m*M* Ni ions, and decreased more strikingly at 5 m*M* Ni ions. These data are consistent with our previous MTT viability studies, which showed that 1 m*M* Ni ions did not cause a significant loss of A549 cell viability (14). Based on these results, we exposed cells to a maximum of 1 m*M* Ni ions in this study.

Effect of Ni Ion Exposure on the Activity of Non-Iron- and Iron (Fe)-Containing Enzymes in Cellular Energy Metabolism. We previously showed that Ni ions decreased the total iron level in A549 cells by about 40% following a 24-hr exposure (7). To assess the

Table 1. Effect of $NiCl_2$ Treatment on the Activity of Multiple Enzymes

Enzyme	Activity (μM/min/mg)[a] Control	$NiCl_2$
Cytoplasmic aconitase	4.3 ± 0.3	0.9 ± 0.1*
Mitochondrial aconitase	1.6 ± 0.1	0.7 ± 0.1*
Succinate dehydrogenase	13.6 ± 1.5	8.9 ± 1.9*
NADH:ubiquinone oxidoreductase	102.8 ± 41.0	55.4 ± 37.3
Mitochondrial isocitrate dehydrogenase	7.6 ± 0.7	11.8 ± 0.6*
Mitochondrial malate dehydrogenase	13.1 ± 1.1	15.0 ± 0.5*
Glutathione peroxidase	6.2 ± 1.1	6.1 ± 0.6

[a] Logarithmically growing A549 cells were treated with 1 m*M* $NiCl_2$ for 24 hrs. Mitochondria were isolated and resuspended in the appropriate buffer. Enzyme activities were measured as described in Materials and Methods.
* Statistically significant change ($P < 0.05$) when compared to control samples.

effect of Ni(II) on cellular iron-dependent processes, we used *in vitro* assays to measure the activity of several Fe-containing enzymes that function in cellular energy metabolism. c-Aconitase activity decreased following a 24-hr Ni ion exposure, reflecting the decreased intracellular iron level (Table 1). Meanwhile, the activities of several Fe-containing enzymes, including m-aconitase, SDH, and complex I, decreased by 40%–50% compared with controls (Table 1). The same Ni ion exposure increased the activities of two Fe-lacking enzymes in the TCA cycle: IDH and MDH (Table 1). Furthermore, Ni ion treatment did not affect the activity of selenium-dependent glutathione peroxidase (Table 1).

Effect of Ni Ion Exposure on Cellular Energy Metabolism. Under physiological conditions, mammalian cells produce ATP mainly through OxPhos, which generates 16-times more ATP than glycolysis. However, when the TCA cycle or OxPhos is blocked, cells are able to greatly upregulate their glycolytic activity in order to maintain a sufficient energy supply. Usually, increased glycolytic activity leads to a higher rate of extracellular glucose consumption and lactate production. Since NADH loses an electron and is converted to NAD^+ primarily in OxPhos, inhibition of OxPhos is expected to cause an accumulation of NAD in its reduced form, NADH, and thus increase the NADH/NAD^+ ratio. To investigate whether these changes in energy metabolism occur in a tissue culture system, a variety of chemical inhibitors of cellular energy metabolism were tested. Carbonyl cyanide p-(trifluoromethoxy)phenyl-hydrazone (FCCP) is an uncoupling agent that dissipates the

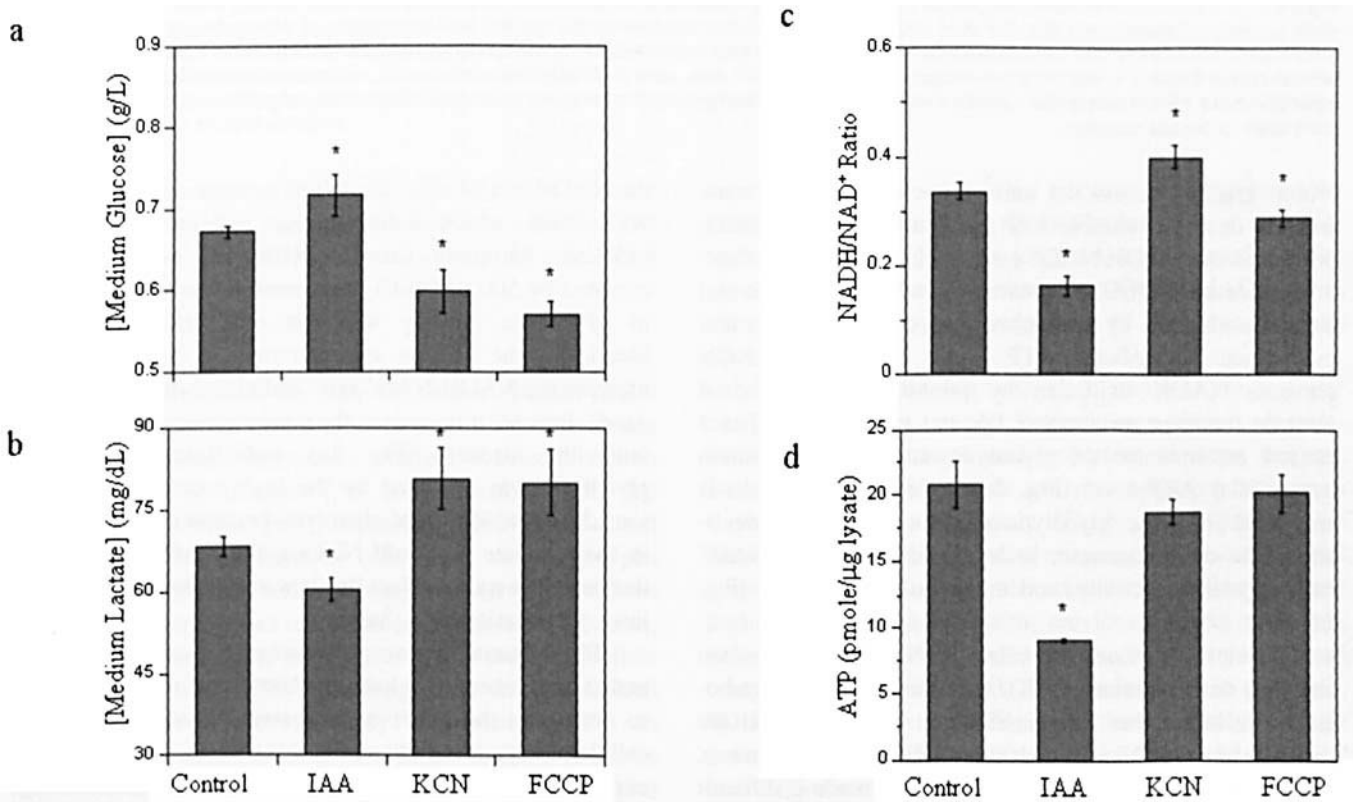

Figure 2. Effect of different chemicals on cellular energy metabolism. Equal numbers of A549 cells were seeded into 6-well plates. Cells were allowed to attach overnight, and then treated with 2 μ*M* iodoacetate (IAA), 500 μ*M* KCN or 5 μ*M* carbonyl cyanide p-(trifluoromethoxy)phenylhydrazone (FCCP) for 4 hrs. After exposure, glucose and lactate concentrations in the medium, the intracellular NADH/NAD^+ ratio, and ATP level were measured as described in Materials and Methods. All measurements were conducted in triplicate. Error bars indicate the standard deviation of three samples with the same treatment. *Statistically significant change ($P < 0.05$) compared to control samples.

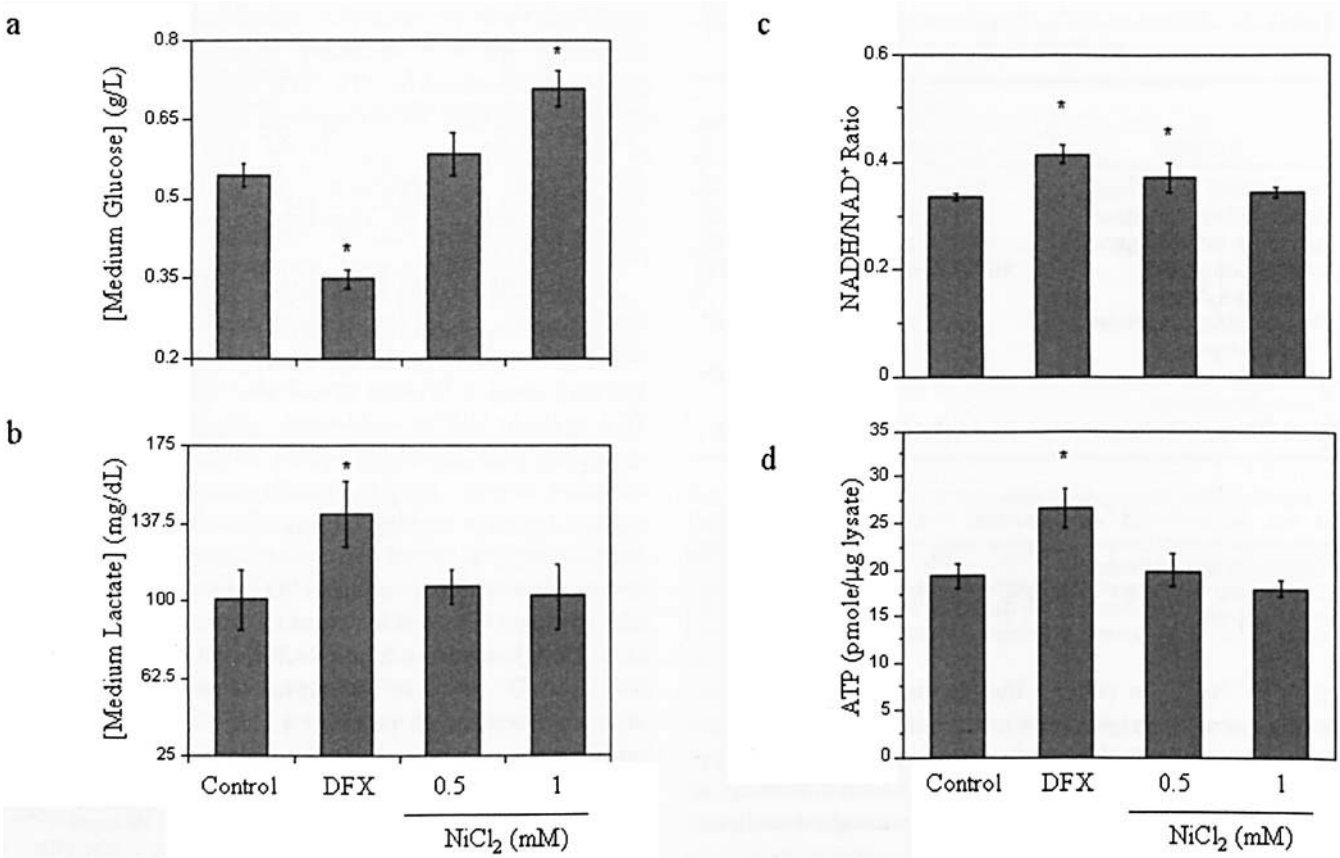

Figure 3. Effect of acute nickel ion exposure on cellular energy metabolism. Equal numbers of A549 cells were seeded into 6-well plates. Cells were allowed to attach overnight and then incubated in serum-free medium for 24 hrs. Medium was replaced with fresh serum-free medium before administration of 100 μ*M* deferoxamine (DFX), 0.5 m*M* $NiCl_2$, or 1 m*M* $NiCl_2$ for an additional 24 hrs. After exposure, the glucose and lactate concentrations in the medium, intracellular NADH/NAD^+ ratio, and ATP level were measured. All measurements were conducted in triplicate. Error bars indicate the standard deviation of three samples with the same treatment. *Statistically significant change ($P < 0.05$) compared to control samples.

proton gradient across the inner mitochondrial membrane and thus decreases aerobic ATP generation. We found that it decreased the NADH/NAD^+ ratio by increasing mitochondrial oxidation of NADH, boosted glucose consumption and lactate production by upregulating glycolytic activity, and maintained intracellular ATP levels (Fig. 2a–d). KCN prevents NADH oxidation by inhibiting mitochondrial electron transport at complex IV, and we observed that it caused an increase of glycolytic activity to maintain intracellular ATP level (Fig. 2a–d). Iodoacetate (IAA) is an inhibitor of the glycolytic enzyme glyceraldehyde 3-phosphate dehydrogenase; it decreased the NADH/NAD^+ ratio, glycolytic activity, and intracellular ATP level (Fig. 2a–d).

We next examined the effect of Ni ions and the iron chelator, deferoxamine (DFX), on cellular energy metabolism. We found that cell proliferation was slowed in the presence of 1 m*M* Ni ions or 100 μ*M* DFX (data not shown), and the resulting disparity in cell numbers made it difficult to interpret glucose consumption and lactate production data. To circumvent this problem, the cell cycle was blocked at the G1 phase by serum starvation prior to treatment. As shown in Figure 3a–d, iron chelation with DFX increased the NADH/NAD^+ ratio, glycolytic activity, and intracellular ATP level, which indicates that cellular OxPhos was blocked. Although the NADH/NAD^+ ratio was also elevated by 500 μ*M* $NiCl_2$ treatment, a subsequent increase in glycolytic activity was not observed (Fig. 3a–d). Increasing the Ni ion concentration to 1 m*M* did not increase the NADH/NAD^+ ratio and glycolytic activity (Fig. 3a–d). Instead, it decreased the consumption rate of glucose from the medium (Fig. 3a), indicating that cellular glycolysis was inhibited by the high concentration of Ni ions. Since inhibition of glycolysis became more prominent in the presence of 1 m*M* Ni ions, the NADH/NAD^+ ratio decreased, despite the fact that it was elevated in 0.5 m*M* Ni ion concentration (Fig. 3a, d).

Since human exposure to nickel is usually chronic in nature and generally at low concentrations, it was important to determine the effect of long-term Ni ion exposure on cellular energy metabolism. For this reason, A549 cells were exposed to a much lower concentration of Ni ions (50–200 μ*M*) for 4 weeks before the effect of Ni ions on cellular energy metabolism was assessed. After 4 weeks' Ni ion exposure, cells acquired an increased NADH/NAD^+ ratio and demonstrated increased rates of glucose consumption

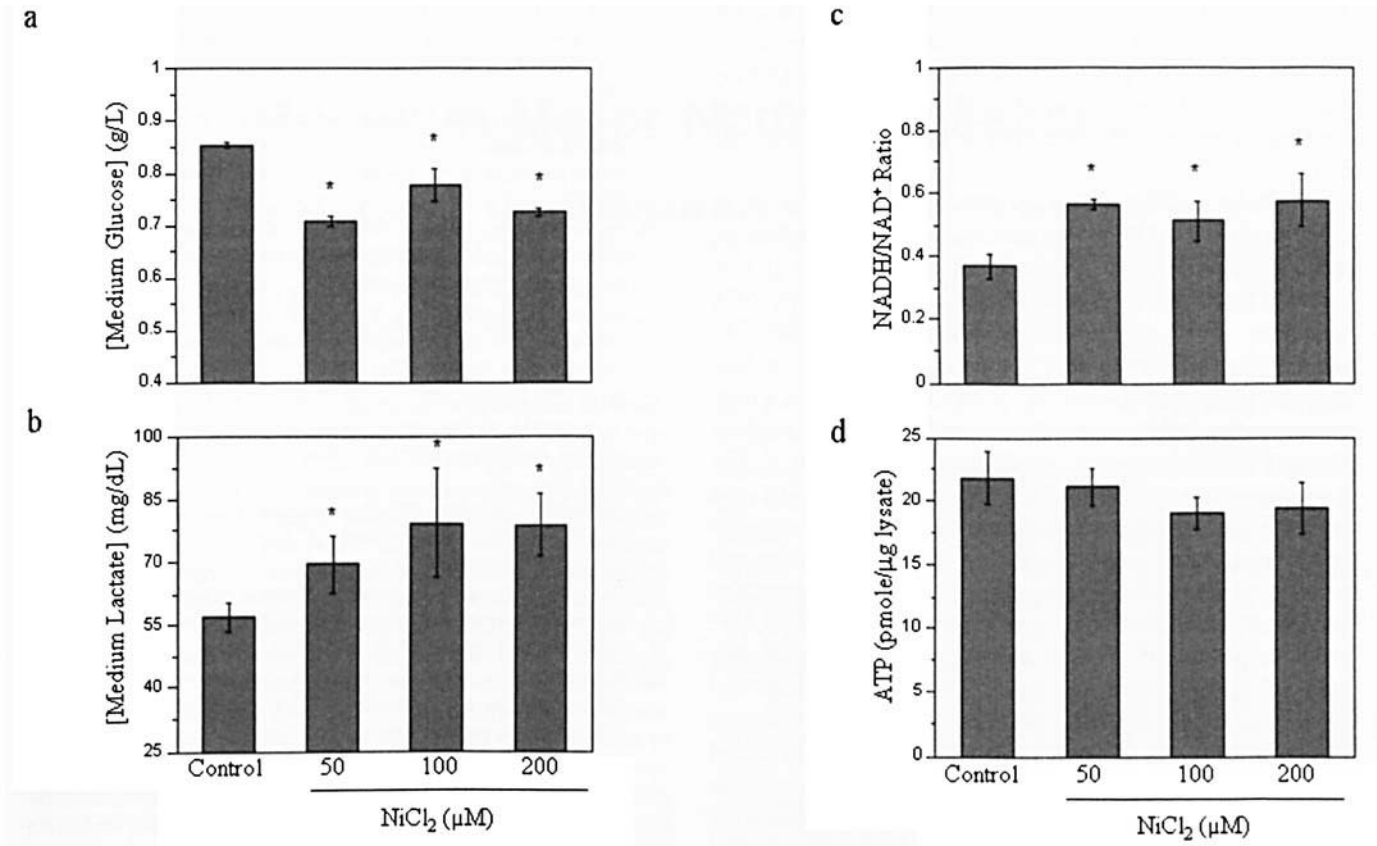

Figure 4. Effect of long-term nickel ion exposure on cellular energy metabolism. A549 cells were exposed to 50–200 μM $NiCl_2$ for 4 weeks. Equal numbers of cells were seeded into 6-well plates. Cells were allowed to attach overnight. Medium was replaced with fresh complete medium containing the indicated concentration of nickel ions and cells were incubated for an additional 24 hrs. After exposure, the glucose and lactate concentrations in the medium, intracellular NADH/NAD^+ ratio, and intracellular ATP level were measured. All measurements were conducted in triplicate. Error bars indicate the standard deviation of three samples with the same treatment. *Statistically significant change ($P < 0.05$) compared to control samples.

and lactate generation (Fig. 4a–d). These results indicate that Ni ion exposure impairs mitochondrial OxPhos, and forces cells to increase glycolytic activity to meet their energy needs.

Discussion

Nickel compounds are harmful to both human health and our living environment (15). Several lines of evidence suggest that nickel compounds interfere with cellular iron metabolism. For instance, Ni ions interfere with the functions of several Fe(II)-dependent dioxygenases and cause a hypoxic condition in cells under normal oxygen tension by stabilizing and activating HIF-1α (16); Ni ions upregulate several genes related to cellular iron metabolism, including TfR and heme oxygenase-1 (17); and iron inhibits nickel subsulfide (Ni_3S_2) carcinogenesis in rat skeletal muscle (18). In our previous study, we reported that Ni ion exposure decreases the level of cellular iron and activates IRP-1 by competing for iron uptake at the divalent metal transporter-1 (7). Here, we further investigated the effect of Ni ion exposure on the functions of several Fe-containing enzymes involved in cellular energy metabolism. Our results demonstrate that Ni ion exposure decreases the activity of these Fe-containing enzymes, and increases the activity of two Fe-lacking enzymes in the TCA cycle. Long-term exposure to Ni ions leads to an increased cellular glycolysis rate and intracellular NADH/NAD^+ ratio, although a higher concentration of Ni ions inhibits glycolysis.

Most Fe-containing enzymes involved in cellular energy metabolism contain Fe-S clusters, which are non-heme prosthetic groups and important electron carriers. Besides its inhibition of c- and m-aconitase activities as shown in our previous study (7), Ni ion exposure also decreases the activities of other enzymes with a similar Fe-S cluster, such as succinate aconitase and complex I. These findings are consistent with previous reports that iron deficiency decreases m-aconitase, succinate aconitase, and complex I activities (20–23). The decrease of m-aconitase, SDH, and complex I activity by Ni ions is likely to result from translation inhibition caused by increased IRE-IRP interactions, as well as destabilization of Fe-S clusters in the enzymes' active centers by iron deficiency. In comparison, Ni ions increase the activities of two Fe-lacking enzymes, MDH and IDH. Since IDH is considered one of the rate-limiting enzymes in the TCA cycle, an increase of its

activity could reflect the cell's effort to restore TCA cycle function following Ni ion exposure. This notion is supported by previous reports that several Fe-lacking mitochondrial enzymes, including IDH and MDH, become activated in rat muscle tissue after an iron-deficient diet (20, 21).

Cellular OxPhos relies on iron for the transfer of an electron from NADH to oxygen. Disruption of OxPhos by iron depletion leads to an accumulation of NADH and an increase in the rate of glycolysis, as was evidenced by DFX treatment. It is still unknown how DFX increases the intracellular ATP level, although a similar finding was also reported by another group (24). It was surprising that a high concentration of Ni ions (0.5–1 m*M*) did not produce changes in cellular energy metabolism similar to DFX. The dose-dependent decrease in the glucose consumption rate indicates that glycolysis is inhibited by a high concentration of Ni ions. After decreasing the Ni ion concentration and prolonging the exposure time, the cells clearly demonstrated increased glycolytic activity and an increased $NADH/NAD^+$ ratio—a pattern of changes similar to those seen during iron-deficiency. Since decreased OxPhos and increased glycolysis are among the fundamental changes undergone by cancer cells (the Warburg effect) and are often associated with an aggressive phenotype and resistance to therapeutic agents (19), the inhibition of OxPhos and activation of glycolysis by Ni ions may play an important role in nickel carcinogenesis.

We thank Jingxia Li for her assistance with ATP measurements and Juliana Powell for her excellent secretarial support.

1. Dallman PR. Biochemical basis for the manifestations of iron deficiency. Annu Rev Nutr 6:13–40, 1986.
2. Wardman P, Candeias LP. Fenton chemistry: an introduction. Radiat Res 145:523–531, 1996.
3. Eisenstein RS. Iron regulatory proteins and the molecular control of mammalian iron metabolism. Annu Rev Nutr 20:627–662, 2000.
4. Metzen E, Ratcliffe PJ. HIF hydroxylation and cellular oxygen sensing. Biol Chem 385:223–230, 2004.
5. Gray NK, Pantopoulos K, Dandekar T, Ackrell BA, Hentze MW. Translational regulation of mammalian and *Drosophila* citric acid cycle enzymes via iron-responsive elements. Proc Natl Acad Sci U S A 93: 4925–4930, 1996.
6. Lin E, Graziano JH, Freyer GA. Regulation of the 75-kDa subunit of mitochondrial complex I by iron. J Biol Chem 276:27685–27692, 2001.
7. Chen H, Davidson T, Singleton S, Garrick MD, Costa M. Nickel decreases cellular iron level and converts cytosolic aconitase to iron-regulatory protein 1 in A549 cells. Toxicol Appl Pharmacol 206:275–287, 2005.
8. Shin AH, Kil IS, Yang ES, Huh TL, Yang CH, Park JW. Regulation of high glucose–induced apoptosis by mitochondrial $NADP^+$–dependent isocitrate dehydrogenase. Biochem Biophys Res Commun 325:32–38, 2004.
9. Ben-Shachar D, Zuk R, Gazawi H, Ljubuncic P. Dopamine toxicity involves mitochondrial complex I inhibition: implications to dopamine-related neuropsychiatric disorders. Biochem Pharmacol 67:1965–1974, 2004.
10. Parker WD, Jr., Parks J, Filley CM, Kleinschmidt-DeMasters BK. Electron transport chain defects in Alzheimer's disease brain. Neurology 44:1090–1096, 1994.
11. Gardner PR, Nguyen DD, White CW. Aconitase is a sensitive and critical target of oxygen poisoning in cultured mammalian cells and in rat lungs. Proc Natl Acad Sci U S A 91:12248–12252, 1994.
12. Zerez CR, Lachant NA, Lee SJ, Tanaka KR. Decreased erythrocyte nicotinamide adenine dinucleotide redox potential and abnormal pyridine nucleotide content in sickle cell disease. Blood 71:512–515, 1988.
13. Jacobson EL, Jacobson MK. Pyridine nucleotide levels as a function of growth in normal and transformed 3T3 cells. Arch Biochem Biophys 175:627–634, 1976.
14. Davidson T, Salnikow K, Costa M. Hypoxia inducible factor-1 alpha–independent suppression of aryl hydrocarbon receptor–regulated genes by nickel. Mol Pharmacol 64:1485–1493, 2003.
15. International Agency for Research on Cancer (IARC). IARC Monographs on the Evaluation of Carcinogenic Risks to Humans, Volume 49. Chromium, nickel and welding. Lyon, France: World Health Organization, IARC, 1990.
16. Salnikow K, Davidson T, Costa M. The role of hypoxia-inducible signaling pathway in nickel carcinogenesis. Environ Health Perspect 110 (Suppl 5):831–834, 2002.
17. Salnikow K, Davidson T, Kluz T, Chen H, Zhou D, Costa M. GeneChip analysis of signaling pathways effected by nickel. J Environ Monit 5:206–209, 2003.
18. Rodriguez R, Kasprzak K. Antagonist to metal carcinogens. J Am Coll Toxicol 8:1265, 1989.
19. Semenza GL, Artemov D, Bedi A, Bhujwalla Z, Chiles K, Feldser D, Laughner E, Ravi R, Simons J, Taghavi P, Zhong H. 'The metabolism of tumours': 70 years later. Novartis Found Symp 240:251–260; discussion 260–264, 2001.
20. Ohira Y, Cartier LJ, Chen M, Holloszy JO. Induction of an increase in mitochondrial matrix enzymes in muscle of iron-deficient rats. Am J Physiol 253:C639–C644, 1987.
21. Cartier LJ, Ohira Y, Chen M, Cuddihee RW, Holloszy JO. Perturbation of mitochondrial composition in muscle by iron deficiency. Implications regarding regulation of mitochondrial assembly. J Biol Chem 261: 13827–13832, 1986.
22. Ackrell BA, Maguire JJ, Dallman PR, Kearney EB. Effect of iron deficiency on succinate- and NADH-ubiquinone oxidoreductases in skeletal muscle mitochondria. J Biol Chem 259:10053–10059, 1984.
23. Oexle H, Gnaiger E, Weiss G. Iron-dependent changes in cellular energy metabolism: influence on citric acid cycle and oxidative phosphorylation. Biochim Biophys Acta 1413:99–107, 1999.
24. Sangchot P, Sharma S, Chetsawang B, Porter J, Govitrapong P, Ebadi M. Deferoxamine attenuates iron-induced oxidative stress and prevents mitochondrial aggregation and alpha-synuclein translocation in SK-N-SH cells in culture. Dev Neurosci 24:143–153, 2002.